EFSUMB Course Book, 2nd Edition

Editor: Christoph F. Dietrich

Parathyroid

Dana-Liana Stoian, Andreea Bena

[1]Clinics of Endocrinology, Department of Internal Medicine, Victor Babes University of Medicine and Pharmacy, Timisoara, Romania

[2]Outpatient Clinics Endocrinology, County Clinic Emergency Hospital, Timisoara, Romania

Corresponding author: Andreea Bena, borlea.andreea@umft.ro

Introduction

Parathyroid ultrasound assessment follows distinct principles compared to the evaluation of most other organs typically accessible by ultrasonography. While high-resolution ultrasound systems are capable of visualizing normal parathyroid glands during real-time cervical scanning, the primary objective of parathyroid ultrasound is different. Morphological evaluation of the parathyroid glands is warranted in patients with a biochemical diagnosis of hyperparathyroidism, be it primary, secondary, or tertiary, and serves predominantly as a first-line imaging modality for localization. This localization is crucial in identifying candidates suitable for minimally invasive surgical intervention. Additionally, parathyroid ultrasound facilitates the assessment of concurrent thyroid pathology, which may significantly influence the overall therapeutic strategy.

According to the current guidelines (1–4), morphological imaging of the parathyroid glands does not contribute to the diagnosis or exclusion of hyperparathyroidism (HPTH). Instead, imaging is reserved for patients with a well-established surgical indication, which includes individuals under the age of 50, those presenting with symptoms, or patients exhibiting impaired renal function, osteoporosis, significant hypercalcemia (serum calcium >11 mg/dL), or elevated urinary calcium excretion—defined as >250 mg/day in women and >300 mg/day in men. Importantly, the ultrasound appearance of the parathyroid glands does not determine surgical eligibility.

Normal parathyroid

The traditional belief by which only abnormal parathyroids can de identified by ultrasound evaluation is no longer valid. Normal parathyroid glands (PTGs) are described as well defined, homogenous, parenchymatous structures, that appear hyperechoic or isoechoic (5), relative to surrounding structures, both thyroid parenchyma and strap muscles [Figure 1] (6).

Figure 1 Oval shaped hyperechoic parathyroid. Right transversal section (a). Round shaped isoechoic parathyroid. Left longitudinal section (b)

a

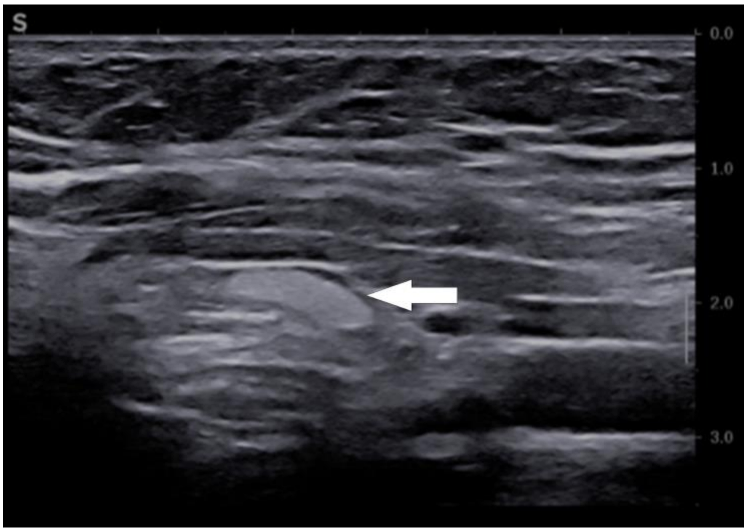

b

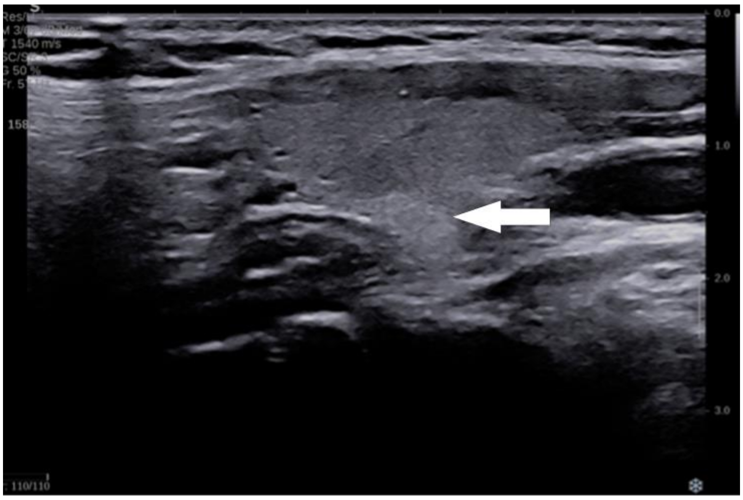

A proportion of parathyroid glands, around 25% in some studies (6), remain undetectable on ultrasound. This limited visibility may be attributed to interindividual variability in adipocyte content. Increased echogenicity has been shown to correlate positively with the fat cell composition of the parathyroid tissue. Indeed, the hyperechogenic appearance of normal parathyroid glands may be attributed to their relatively high adipose content, which constitutes approximately 35 - 50% of the glandular tissue (7).

Data in the literature defines normal size of parathyroid glands, with no significant differences in volume with respect to age, with a mean size of 6.6 ± 1.4/ 4.8 ± 1.1/ 3.6 ± 0/8 mm, slight bigger in males than in females: volume of 69.8 ± 36.9 mm^3 versus 60.0 ±30.6 mm^3 (5,8). Shape: The vast majority of the normal parathyroid glands are round or oval [Figure] (5,6,8), teardrop shape or irregular shape being observed in 2.2%, respectively 2.5%. Orthotopic position of the parathyroids is described in around 94% of cases (87.4-98.6%) (9) but hyperparathyroidism patients, the prevalence of ectopic location is higher, with 12.3% neck and 5.2% mediastinum locations, as observed in a recent published meta-analysis comprising more the 7000 cases, ectopic left lower parathyroid being the most frequent non-orthotopic location (10). Only 1.25% of orthotopic parathyroids are located inside the thyroid capsule [Figure 2].

Figure 2 Oval shape, isoechoic right superior parathyroid (white arrow) inside the thyroid capsule (gray arrow). Right transversal section.

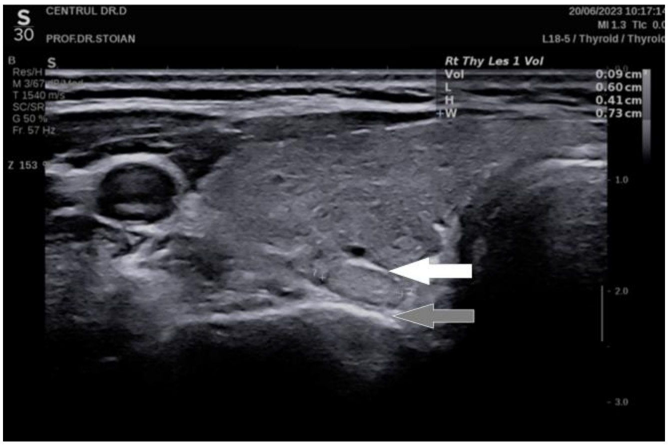

Regarding anatomical distribution, normal parathyroid glands are most commonly visualized in the region of the lower thyroid pole and the infrathyroidal space. In our study, 66% of identifiable glands were located in this area, likely due to their more superficial positioning and the enhanced sonographic contrast provided by the surrounding structures (6,8,11). Superior and middle parathyroid glands are frequently positioned in deeper anatomical regions, particularly within the tracheoesophageal groove. This deeper location can hinder their identification on ultrasound when compared to inferior glands, often necessitating adjustments in scanning technique to improve detection. There are situations in which all for parathyroids identifiable on ultrasound [Figure 3 a-d].

Figure 3 Right superior PTG (transverse and longitudinal right section) (a). Right inferior PTG depicted extrathyroidal, postero-caudal to thyroid caudal pole (transverse

and longitudinal right section) (b). Left superior PTG depicted extrathyroidal, postero-caudal to the left thyroid lobe, adjacent to the caudal thyroidal pole (transverse and longitudinal right section) (c). Left inferior PTG depicted below the left thyroid lobe, in the esophageal grove (transverse and longitudinal right section) (d).

a

b

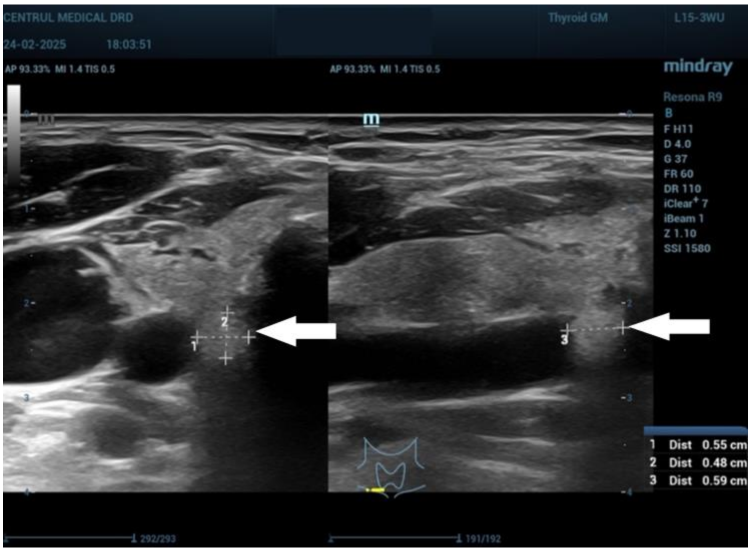

c

d

Parathyroid pathology

Congenital anomalies such as agenesis or hypoplasia, cannot be evaluated by ultrasound, nor by any other imaging modality, the diagnostic being biochemical in cases of congenital hypoparathyroidism defined by hypocalcemia and low levels of calcitriol, because of PTH insufficiency. Ectopic or supernumerary parathyroid localizations are not clinically relevant under normal circumstances, only in cases with hyperparathyroidism where definitive treatment is needed (9). Hypertrophic or hyperplasic parathyroid tissue has a different morphology compared with the physiological parathyroid. Parathyroid adenomas and hyperplastic glands are characterized by a marked increase in the number of chief cells (12,13). Due to their uniform cellular architecture and the relatively small size of chief cells compared to adipocytes, most ultrasound waves encounter the tissue at non-perpendicular angles, resulting in significant scattering. As a consequence, only a minimal portion of the acoustic signal is reflected back to the transducer, leading to a hypoechoic appearance on ultrasound imaging (14) being hypoechoic compared to the thyroid parenchyma [Figure 4], in contrast to normal parathyroids, which, if visible, are always iso- or hyperechoic (5).

Figure 4 Right inferior physiological PTG - round, hyperechoic relative to the thyroid parenchyma, with right superior PTA -oval, inhomogeneous, hypoechoic relative to the thyroid parenchyma (longitudinal section of the right thyroid lobe – RTL).

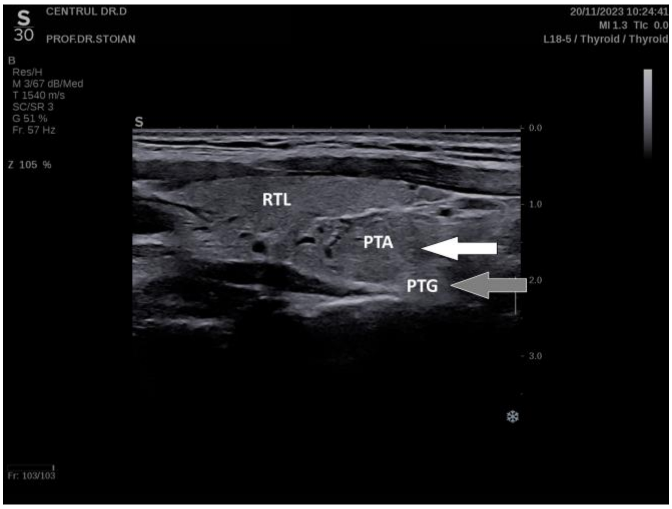

In addition to the typical oval morphology, parathyroid adenomas (PTAs) may present with a variety of atypical shapes. These include flat (12.6%), kidney-shaped (7.8%), triangular (15.6%), dacryoid (8.4%), and round (3%) configurations. Overall, approximately 11.4% of adenomas exhibit atypical morphological features (15). The most commonly described morphological variants of parathyroid adenomas [Figure 5 to 11].

Figure 5 Left superior PTA – oval shape, mild hypoechoic, well defined homogenous (left longitudinal section).

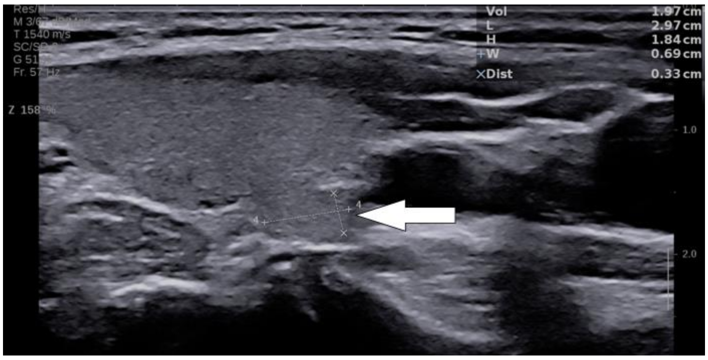

Figure 6 Triangular left superior PTA (left transverse section).

a

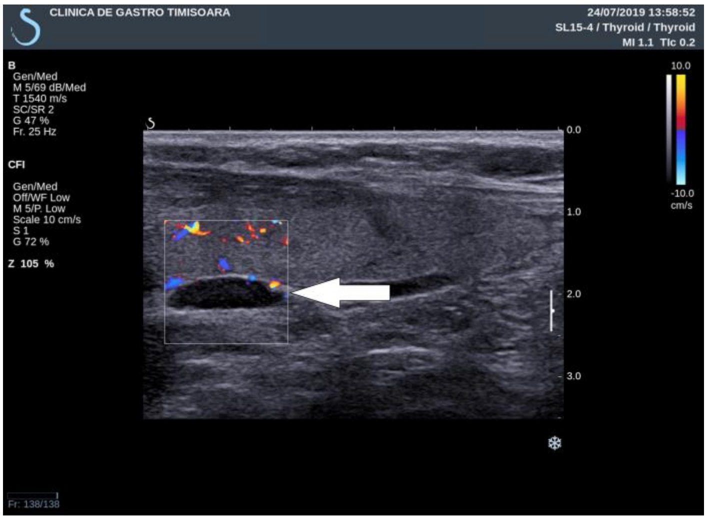

b

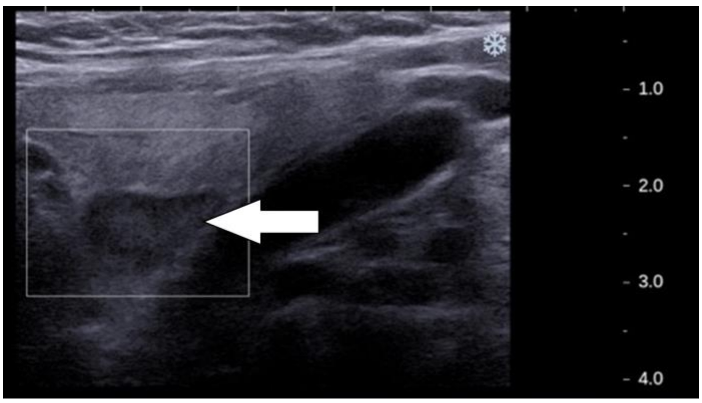

Figure 7 **Left thyroid lobe, occupied by a TIRADS 5 thyroid nodule (arrow) with extrathyroidal locate PTA, intense hypoechoic with flat appearance (dashed arrow) (transverse section).**

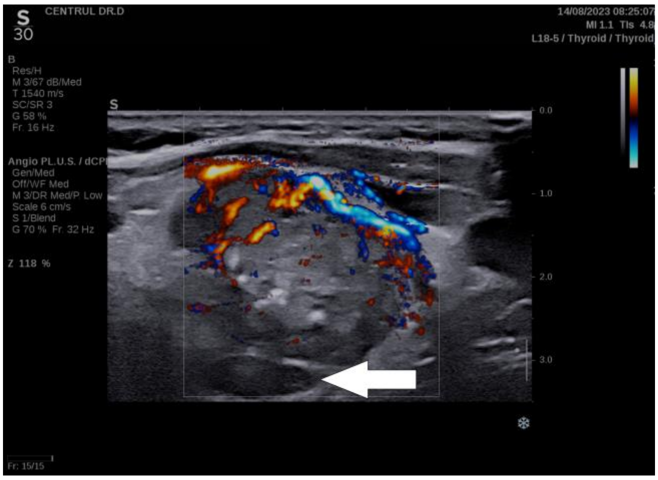

Figure 8 **Left PTA – Polylobate right superior PTA (arrow) (left transverse section).**

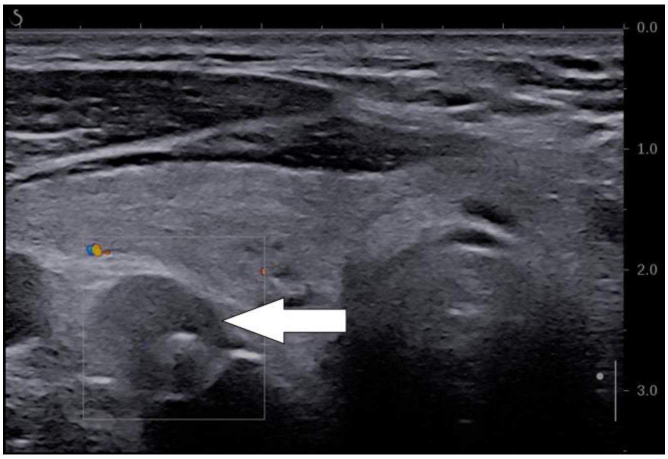

Figure 9 **Dacroid (eye drop) right PTA extrathyroidal location, intense hypoechoic homogenous appearance. CDUS Typical feeding artery (right transverse section).**

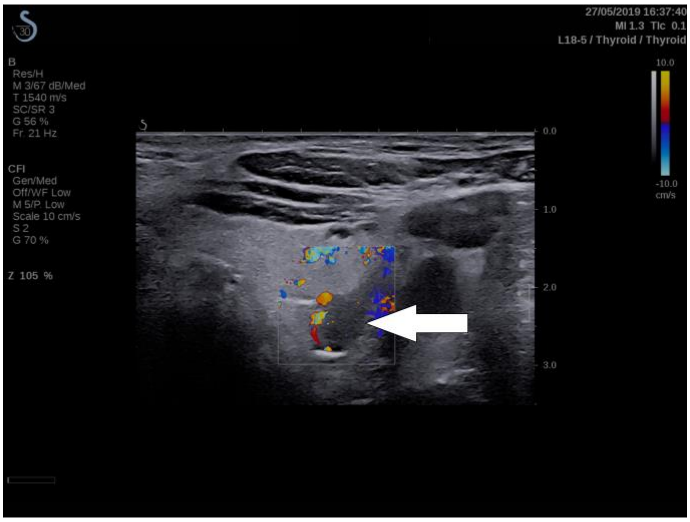

Figure 10 **Left PTA – Pseudo kidney shape, extrathyroidal location, intense hypoechoic appearance (longitudinal section).**

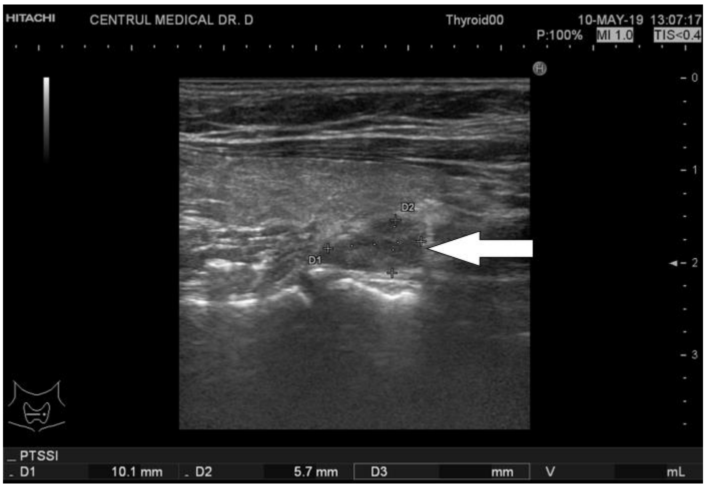

Figure 11 Right superior PTA, intense hypoechoic, inhomogeneous round shape.

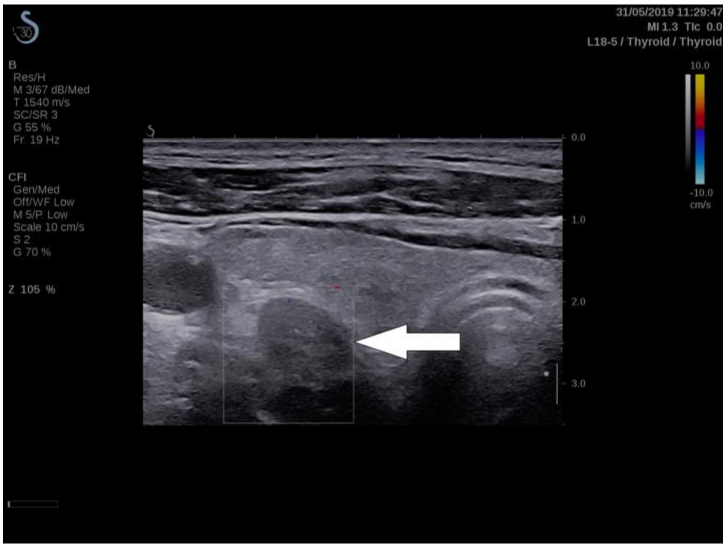

In patients with a confirmed diagnosis of hyperparathyroidism (HPTH), the disease is, in the vast majority of cases, sporadic in nature, reflecting its known epidemiological profile (11). Approximately 90% of cases are attributed to a single parathyroid adenoma, while double adenomas account for 2–5% of cases as illustrated in [Figure 12]. Atypical locations require confirmation through second-line morphological assessment, with current guidelines generally recommending scintigraphy or SPECT (3,4), as seen in [Figure 13]. Multiglandular disease may be observed in up to 20% of patients. Cystic adenomas and parathyroid carcinomas represent rare entities, with reported frequencies of approximately 3% [Figure 14], and less than 1%, respectively.

Figure 12 67-year-old women, primary hyperparathyroidism. Adjacent and parallel to both thyroid lobs, hypoechoic, oval, well defined parenchymatous structures confirmed as parathyroid tissue both by scintigraphy and neck MRI. Right PTA -

right transverse section (a). Right PTA - right longitudinal section (b). Left PTA - left transverse section (c). Left PTA - left longitudinal section (d).

a

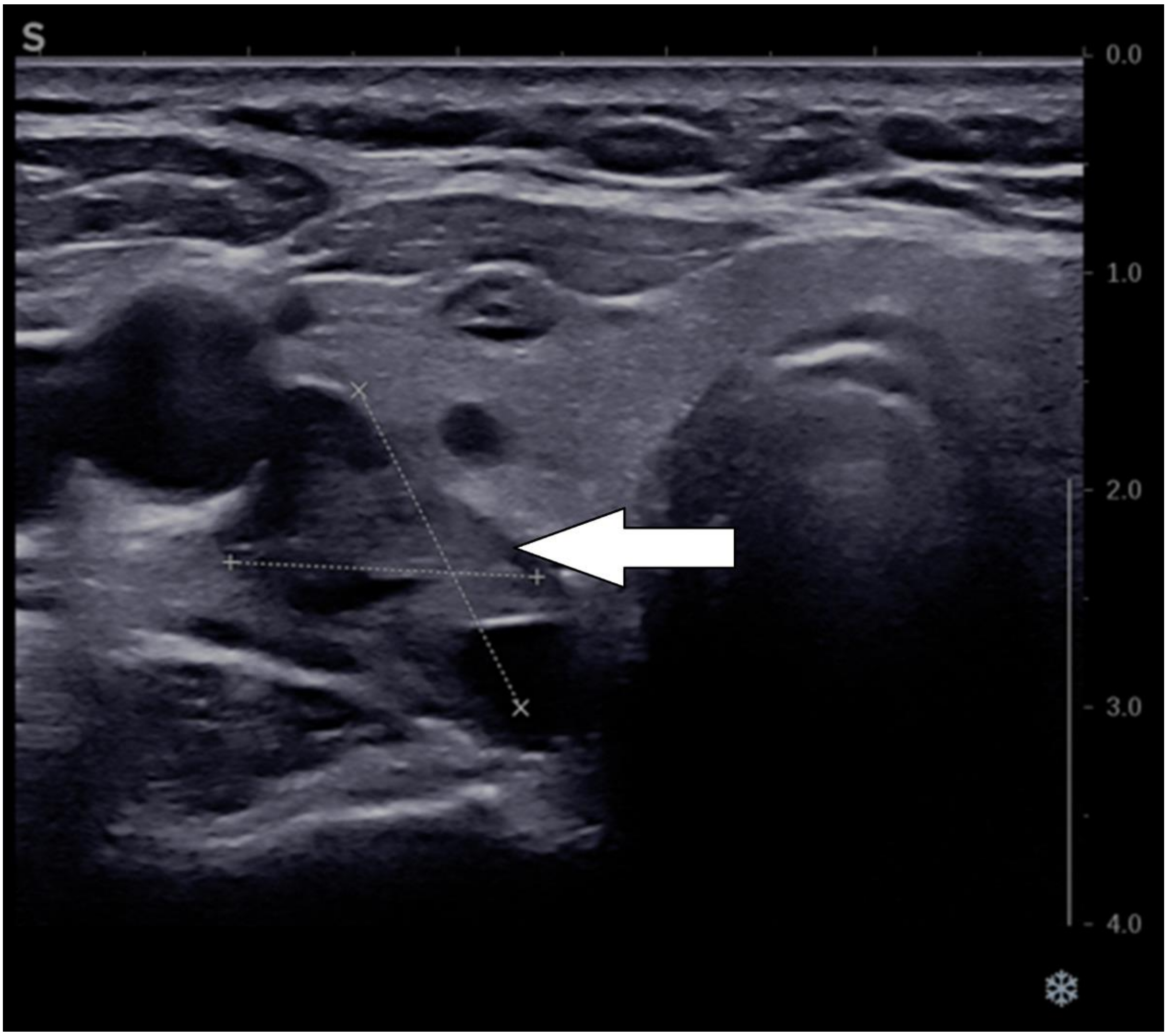

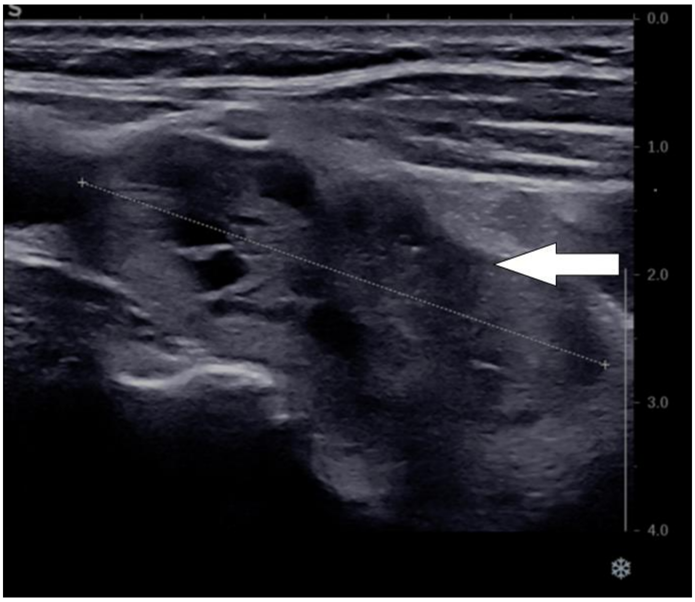

c

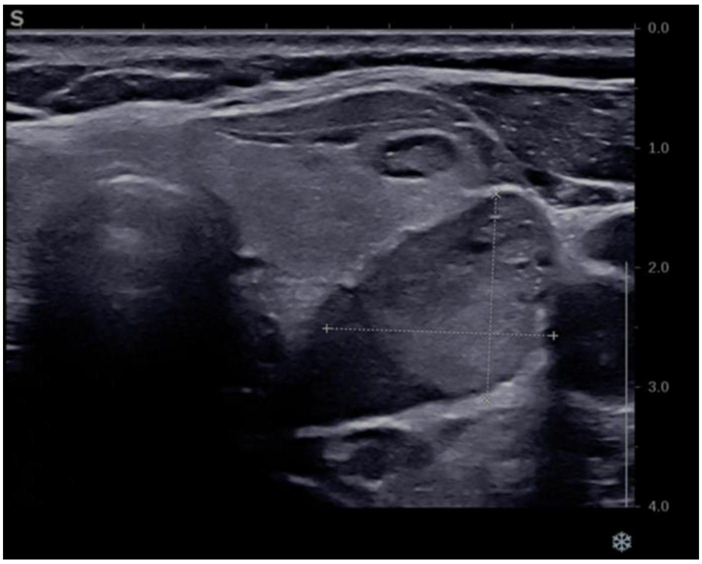

d

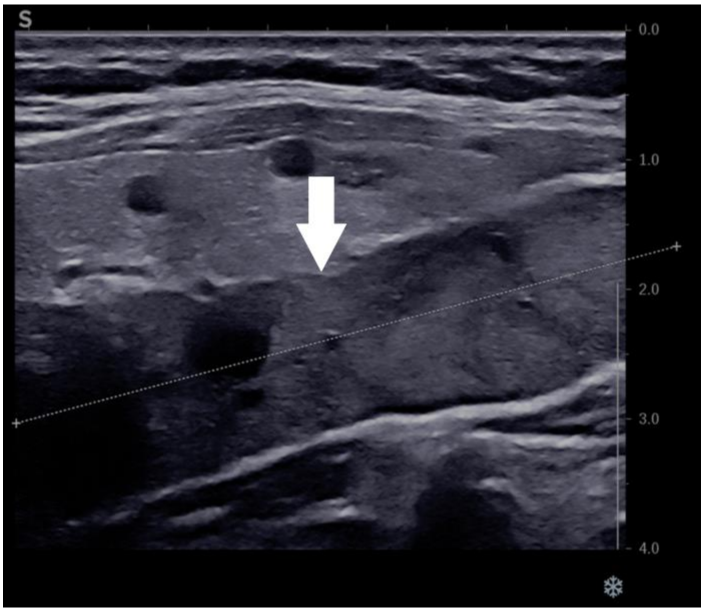

Figure 13 **Sesta-MIBI Scintigraphy, parathyroid exposure time (90’ and 120’after the administration of radiotracer) reconfirming both sided activity/uptake consistent for parathyroid hyperactive tissue.**

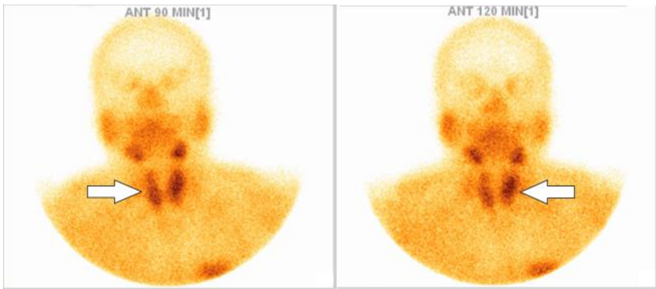

Figure 14 **Cystic right inferior PTA (white arrow) with typical Blue-Green-Red artifact, reemphasizing the fluid content (gray arrow) (longitudinal right section).**

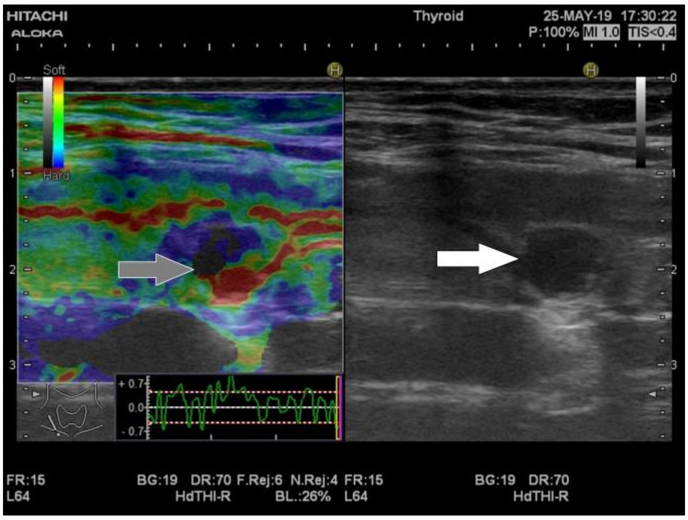

As physiological parathyroids, PTA cand be also located extra or intracapsular, complete intrathyroidal position being possible (16).

Figure 15 **Right inferior PTA, extracapsular location (longitudinal right section) (a). Right superior PTA, intracapsular location (transverse right section) (b).**

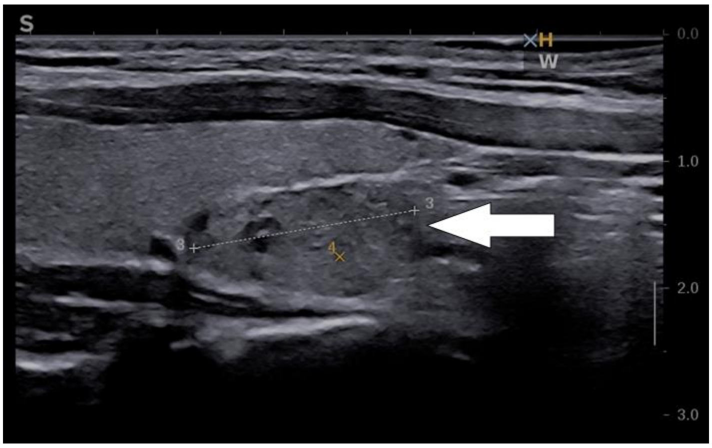

b

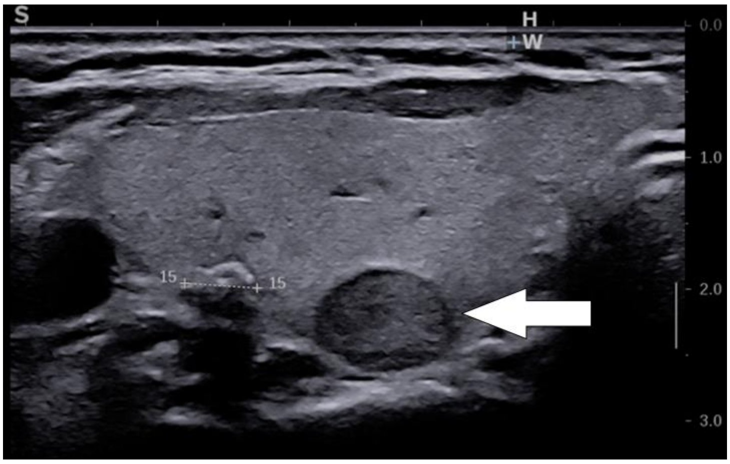

Parathyroid lesions usually exhibit increased blood flow on color Doppler, often presenting a combined pattern of peripheral and intralesional hypervascularity. In some cases, a distinct feeding artery supplying the abnormal gland can be visualized (17) [Figure 16]. In addition to the presence of a feeding artery, the most frequently reported Doppler patterns in parathyroid adenomas include a peripheral rim of vascularity [Figure 17] or asymmetrically increased blood flow as displayed in [Figure 18] (18–20).

Figure 16 Right superior PTA with feeding artery (longitudinal right section).

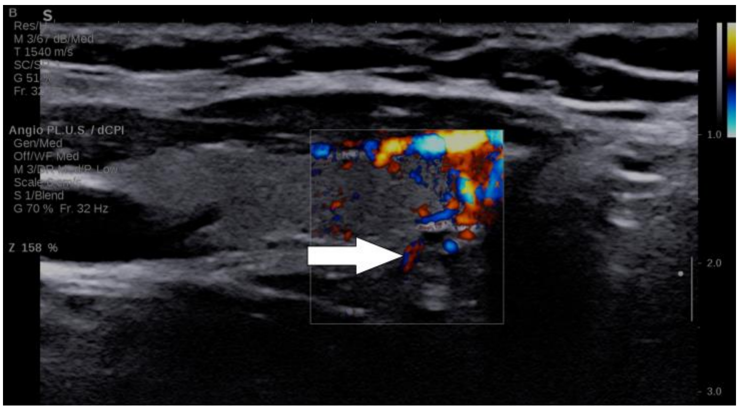

Figure 17 Left superior PTA with peripheral rim vascularization (transverse left section).

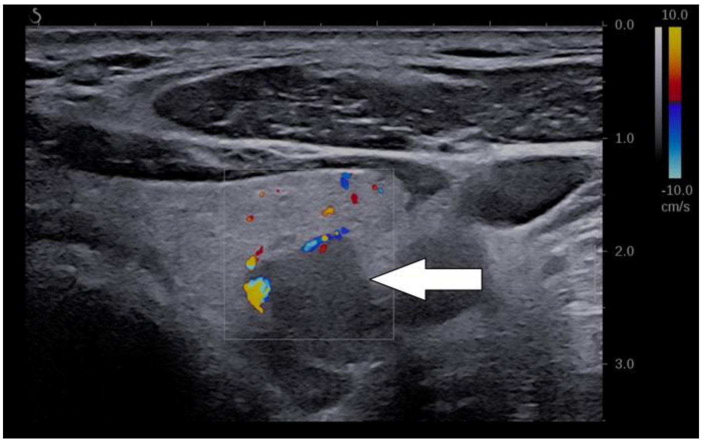

Figure 18 Right PTA with asymmetrical blood flow (longitudinal right section).

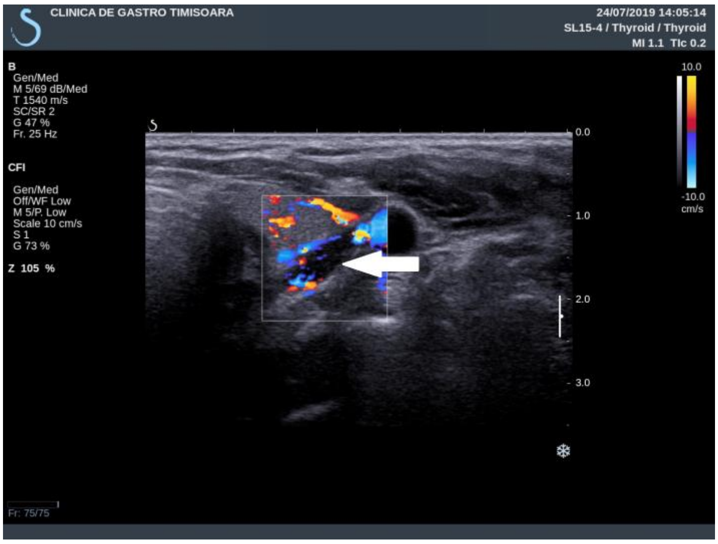

Color Doppler ultrasound demonstrated high diagnostic performance for parathyroid adenoma, with reported sensitivity, specificity, and overall accuracy of 97%, 100%, and 98.6%, respectively. When CDUS findings were integrated with grayscale ultrasound evaluation, the sensitivity for detecting parathyroid adenomas and differentiating them from other cervical lesions such as lymph nodes [Figure 28], muscle tumoral masses [Figure 34b], or branchial cysts [Figure 31], reached 97%, while specificity remained at 100% (19–21).

Parathyroid lesions are described as elastic in the literature, regardless of the type of elastographic technique used (22–25). Research in the field of primary hyperparathyroidism has identified varied threshold values for parathyroid adenomas, contingent upon the elastography technique utilized. A cut-off of 9.58 kPa was determined in our prior investigations to differentiate parathyroid tissue from normal thyroid tissue (26). Shear Wave Virtual Touch Imaging Quantification revealed elevated values for parathyroid adenomas (2.16 ± 0.33 m/s) in contrast to parathyroid hyperplasia (1.75 ± 0.28 m/s), establishing a cut-off value surpassing 1.92 m/s for parathyroid adenomas (23). Utilizing the same elastography technique, a separate study compared parathyroid adenomas with thyroid tissue, determining that the shear wave velocity for parathyroid adenomas was lower than that of thyroid tissue (2.01 m/s versus 2.77 m/s, respectively) (27). Other authors described a threshold of less than 8.9 kPa for parathyroid compared to thyroid tissue, irrespective of the etiology (22,28,29). To distinguish between nodular lesions originating from the thyroid or muscle tissue and parathyroids, the optimal cut-off of less than 9.24 kPa was described. The location of the parathyroid adenoma has no impact on the SWE measurements: anterior adenomas: mean SWE 4.74 ± 2.75 kPa, SWEmax 11.45 ± 6.19 kPa, and SWE-min 1 ± 1.74 kPa; posterior adenomas: mean SWE 4.66 ± 2.88 kPa, SWEmax 11.62 ± 6.94 kPa, and SWE-min 0.80 ± 1.42 kPa(22). The discriminatory differences remained even in cases with associated autoimmune thyroid disease (AITD), with a SWE ratio of 0.418 ± 0.230, in parathyroid adenoma compared to healthy thyroid tissue, as opposed to the value of 0.416 ± 0.186, $p = 0.570$, in parathyroid adenoma compared to AITD tissue (29,30).

Most cases of primary hyperparathyroidism exhibited values ranging from 3.3 to 5.8 kPa (25-75% IQR) [Figure 19], while secondary hyperparathyroidism values ranged from 6 to 8.4 kPa, benign thyroid nodules displayed values between 12.2 and 18.8 kPa [Figure 20], while malignant thyroid nodules ranged from 30.1 to 48.8 kPa (22,28). The ROC curve demonstrates that the optimal cut-off value for parathyroid adenoma is below 5.96 kPa (26). Consequently, the distinctions between primary and secondary hyperparathyroidism are underscored when there is uncertainty.

Figure 19 **Primary HPTH: Right PTA with a mean elasticity of 2.4 kPa, and a maximum elasticity of 6.8 kPa (left transverse section).**

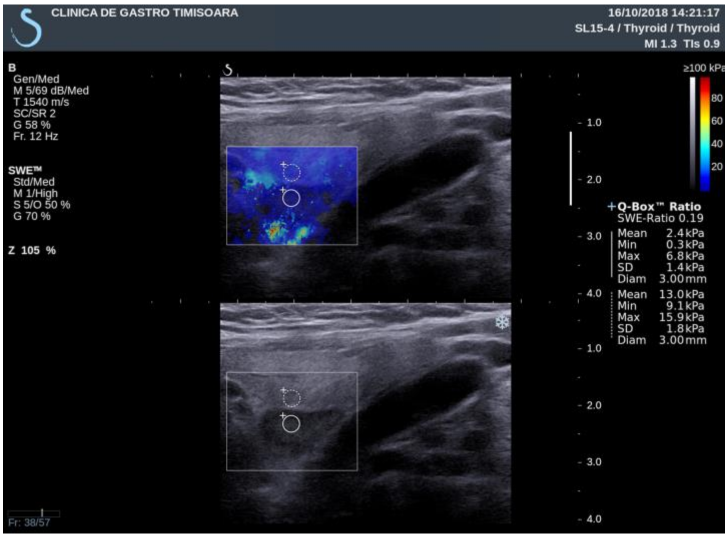

Figure 20 **Superior left hyperplastic PTG, oval, hypoechoic, elastic, with mean elasticity of 7.3 kPa (a)**. **Superior left hyperplastic PTG, oval, hypoechoic, elastic, with mean elasticity of 8.2 kPa (b)**.

a

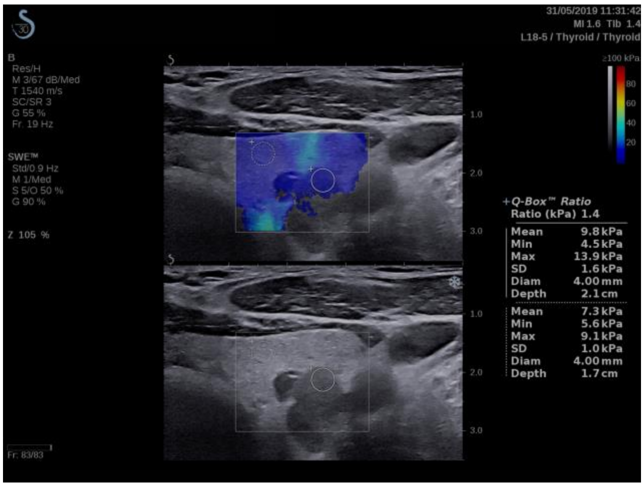

b

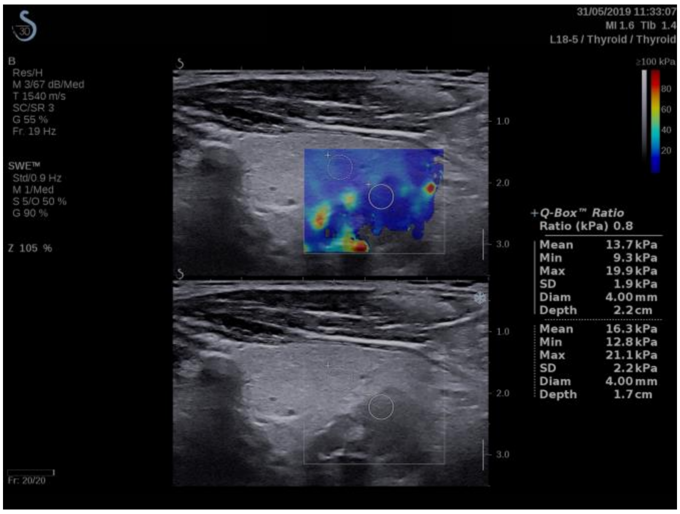

CEUS of parathyroid lesions demonstrates efficacy in distinguishing adenoma from hyperplasia, irrespective of the volume of contrast material administered. The quantitative analysis enhanced the sensitivity and specificity in distinguishing parathyroid lesions. Hyperplasia exhibited uniform enhancement, rapid uptake, and a consistent wash-out look; adenoma was identified by peripheral uptake, central wash-out, and diminished hemodynamics. Employing CEUS quantification techniques is recommended to enhance the ultrasound diagnostic capability for suspected parathyroid abnormalities (31). But from the clinical point of view, adenoma or hyperplasia becomes relevant only in cases with confirmed primary hyperparathyroidism, with surgical indication due to age of the patient or end-organ complications, such as bone or kidney. In CEUS assessment, parathyroid hyperplasia is distinguished by rapid, intense, homogenous enhancement and a uniform wash-out appearance, while adenomas exhibit early peripheral hyperenhancement with central wash-out in the later phases [Figure 21] (31,33,34). Moreover, CEUS helps in differentiation of parathyroid structures with lymph nodes, with homogenous enhancement in adenopathy versus inhomogeneous distribution of the bubbles in PTA [Figure 22] (31).

Figure 21 Right inferior PTA position – infrathyroidal, solid, homogenous hypoechoic, with centripetal wash-in pattern (transparent arrow).

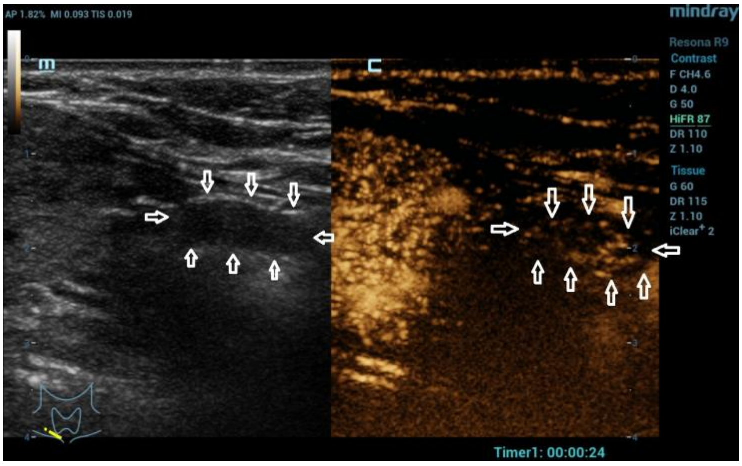

Figure 22 Parathyroid adenoma with inhomogeneous intralesional distribution (transparent arrow), compared with intense homogenous distribution in a lymph node (gray arrow).

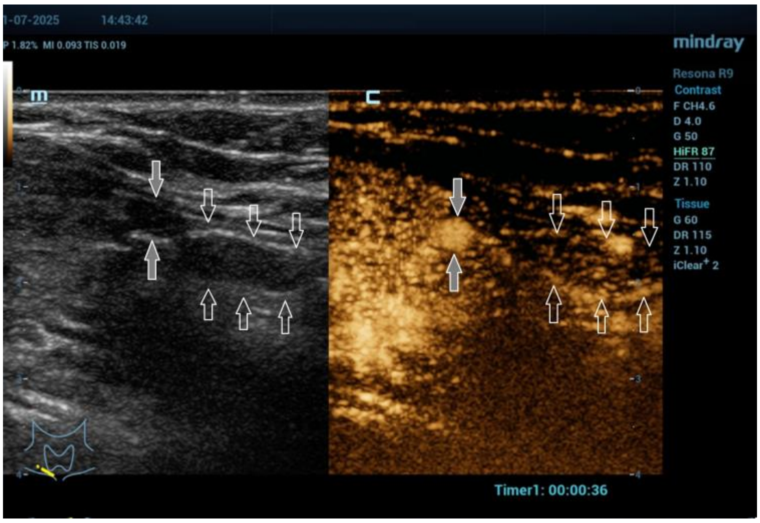

At present, ultrasound criteria capable of reliably differentiating parathyroid carcinoma from benign parathyroid tumors are not well established in the literature. Nevertheless, certain sonographic findings may raise suspicion for malignancy, including a lesion length exceeding 3 cm, a depth-to-width ratio greater than 1, a lobulated hypoechoic or heterogeneous echotexture, irregular margins, a thick capsule, abnormal vascularity, and the presence of intranodular calcifications (19,35), [Figure 23 c], as compared to smooth hypoechoic homogenous parenchymatous structures, as in PTG [Figure 23 a], respectively with slight inhomogeneous pattern in atypical PTA [Figure 23 bb]. It is important to note, however, that these characteristics can also occur in benign lesions, making them insufficient for a definitive preoperative diagnosis. In some cases, infiltration of adjacent structures or enlargement of cervical lymph nodes may be detected or suspected (36). Integration of both morphological and functional data can add diagnostic power in differentiation of parathyroid carcinoma cases (37). From the multimodal US evaluation point of view, the maximum shear wave velocity and Young's modulus exhibit superior sensitivities of 0.75 and 0.81, with cut-of values of 2.35 m/s and 17.05 kPa, respectively in the differential diagnostic of parathyroid carcinoma. The "colored lesion" and "stiff rim" patterns on the elastogram are more indicative of parathyroid carcinoma and atypical parathyroid tumours, while a negative elastogram is predominant in parathyroid adenoma. Even parathyroid cancers which are stiffer than PTA have a mean elasticity around 17-18 kPa (38).

Figure 23 **The typical ultrasound presentation of a parathyroid neoplasm: Homogeneous hypoechoic reflectivity with oval shape of a typical PTA (a)**, **heterogeneous with microcalcification appearance of a parathyroid carcinoma (b)** and **mixed echotexture slight heterogenous of an atypical adenoma (c)**

a

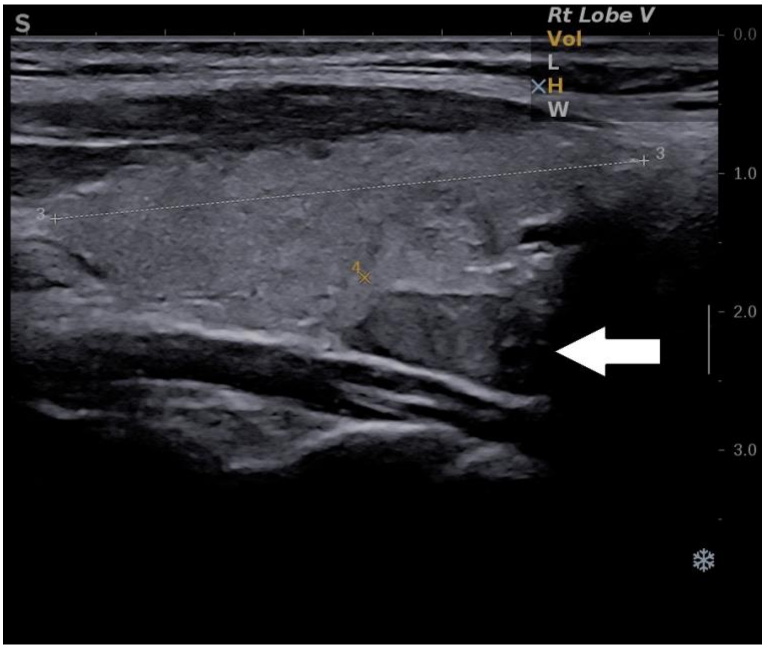

b

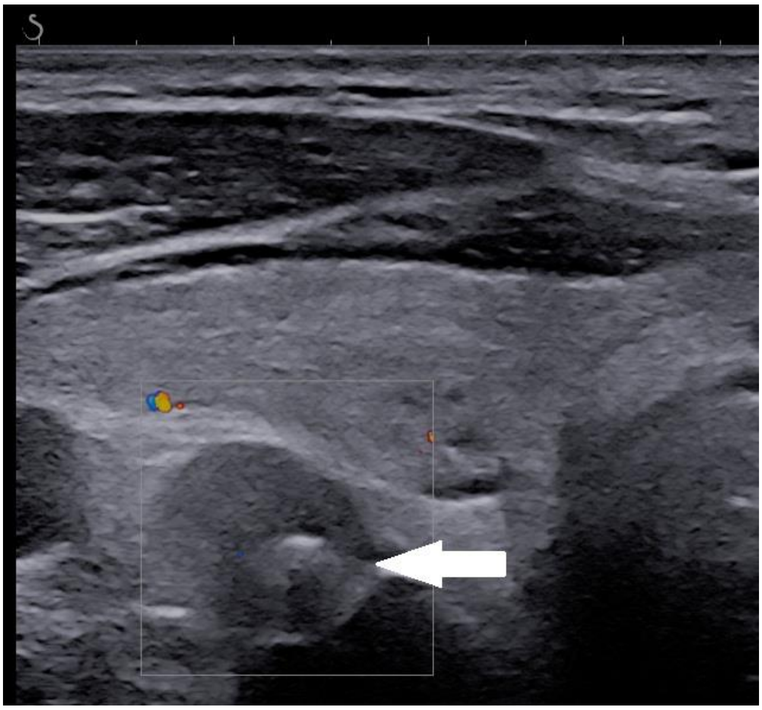

c

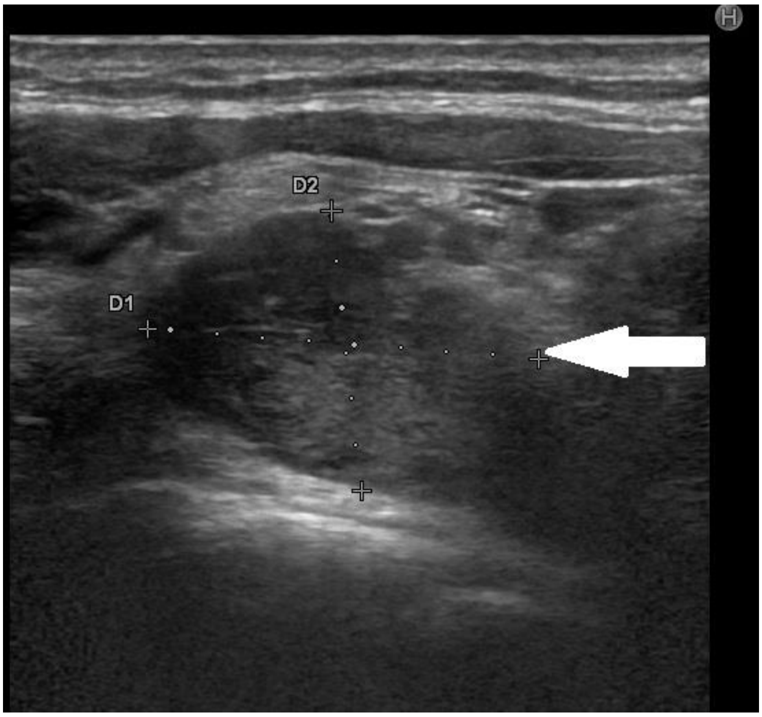

US limitations are related to high body mass index, with deeper parathyroid location due to subcutaneous fat layer, variability of the disease, mainly cystic appearance as depicted in [Figure 14] very small in size parathyroids, posterior located glands, false positive from thyroid pathology, intrathyroidal located parathyroids [Figure 24] and, off course ectopic glands (9,15,39) and the presence of different neck masses than cam mimic parathyroid pathology.

The identification of **intrathyroidal PTG** [Figure 24a] can be challenging, both with oval/round shaped hypoechoic appearance [Figure 24b], but the vascular pattern, mainly the typical feeding artery (18,21) [Figure 24c] and elasticity [Figure 24d] of the parathyroid adenoma (22,26) can be suggestive for the correct diagnostic. When no extrathyroidal parathyroid adenoma is identified, the presence of a nodule displaying these features in a patient with strong clinical and biochemical evidence of hyperparathyroidism should prompt increased consideration of an intrathyroidal parathyroid adenoma.

Figure 24 Oval/kidney shaped marked hypoechoic PTA with intrathyroidal location (right transverse section) (a). Oval/kidney shaped marked hypoechoic PTA with

intrathyroidal location (right transverse section) (b) with feeding artery cranial position (c) and **very soft in 2D-SWE elastography (d)**.

a

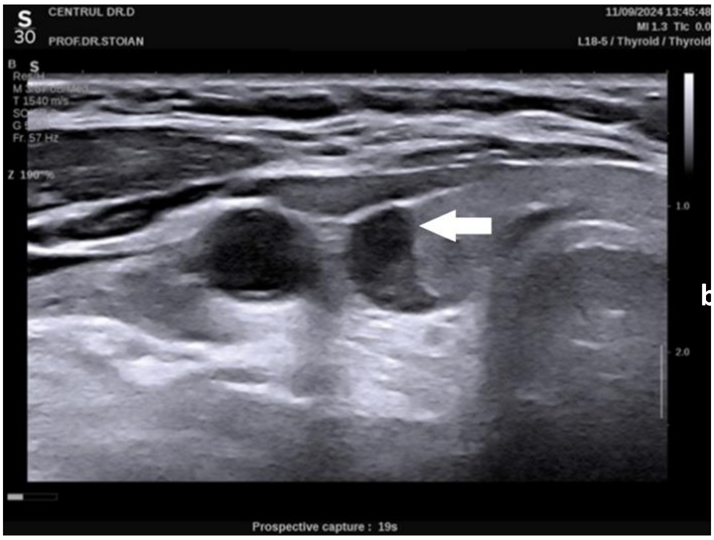

b

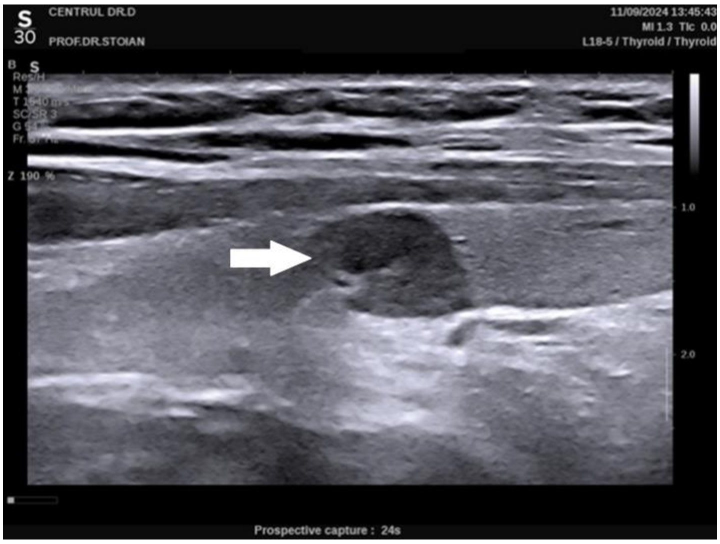

c

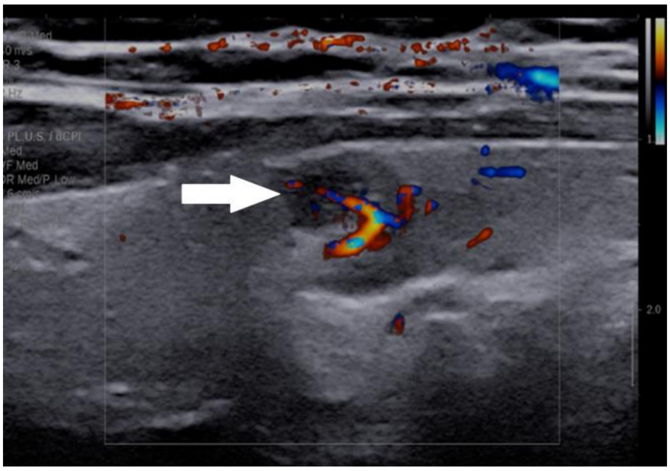

d

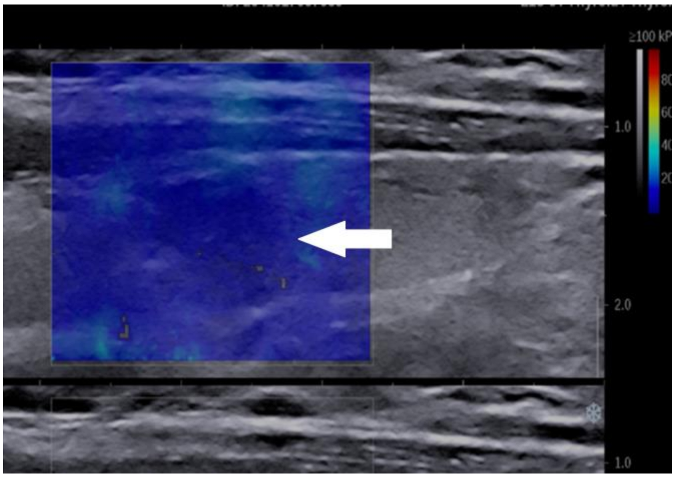

The prevalence of **concomitant thyroid nodules** in individuals with primary hyperparathyroidism (PHPT) has been reported to vary considerably across studies, with figures ranging from 18% to 85% (40,41) while in patients with secondary hyperparathyroidism due to end-stage renal disease, the rate is approximately 62% (42). The nature of the association between PHPT and thyroid pathology remains unclear and is likely influenced by multiple factors (40). Accurate localization of abnormal parathyroid tissue using preoperative imaging is a key determinant of surgical success. Advances in diagnostic technology have facilitated the adoption of a multiparametric ultrasound (US) strategy, enhancing lesion characterization, improving diagnostic precision, and increasing the clinical value of ultrasound. In addition to traditional B-mode and Color Doppler imaging, this comprehensive US approach integrates contrast-enhanced ultrasound (CEUS) and elastography as part of the multimodal evaluation pathway. When evaluation conventional

US characteristics, individual parameters, such as non-oval shape, marked hypoechogenicity and intranodular vascular signals all distinguished parathyroid nodules from concomitant thyroid nodules (15). A cut-off value of ≤9.24 kPa for the 2D SWE PLUS method has been determined for differentiating parathyroid [Figure 25b] and thyroid nodules [Figure 25a]. The diagnostic performance at this threshold exhibited a sensitivity of 94.2%, specificity of 91.1%, negative predictive value (NPV) of 93.5%, and positive predictive value (PPV) of 92%.

When looking whether significant differences exist between the cancer subgroups and parathyroid tissue, considering the various subtypes of thyroid malignancy, a lower EI value lower than the predefined cut-off of 9.24 kPa, a marked difference was observed between papillary thyroid carcinoma and parathyroid lesions, with PTA with the lowest elasticity 3.5-5.8 kPa [Figure 26b], followed by NIFT-P pathology, 21.6 kPa, medullary thyroid carcinoma, with a mean elasticity index of 27.4 kPa, follicular thyroid cancer 47.7 kPa, with papillary thyroid carcinomas (PTC) [Figure 26a] the stiffest of all nodular pathologies, with 37.7 kPa (32.5-52.9 median 25 -75 IQR) (28).

Figure 25 Central thyroid nodule – TIRADS 4 - follicular adenoma at pathology report with E mean = 30.9kPa - 2DSWE, right longitudinal section with (a) right PTA, E Mean = 22 kPa - 2DSWE, right longitudinal section with (b).

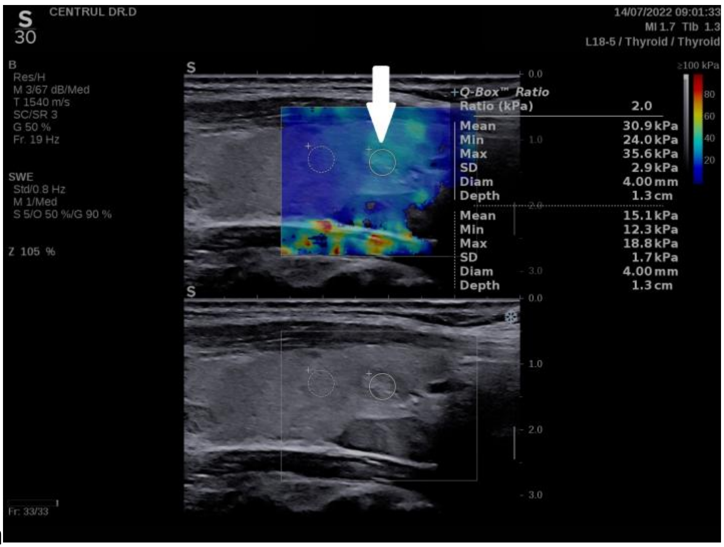

a

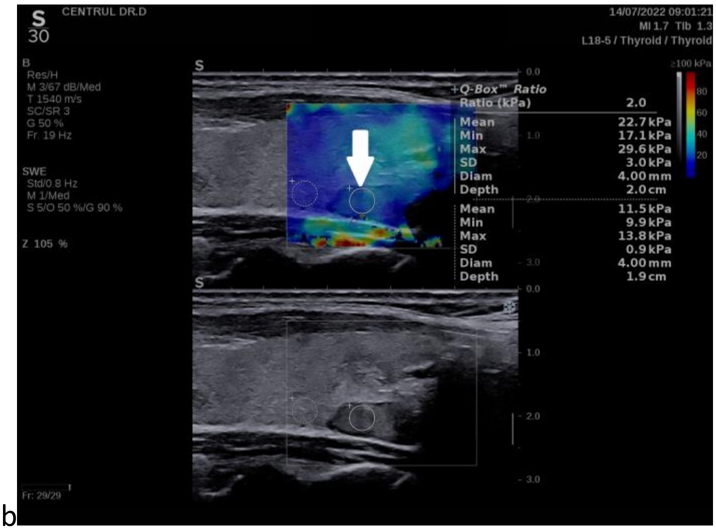

b

Figure 26 TIRADS 5 right thyroid nodule - PTC (pathology report) with E mean = 70.8kPa, transversal right section (a). R**ight PTA, E Mean = 6 kPa - 2DSWE, transversal right section (b)**.

a

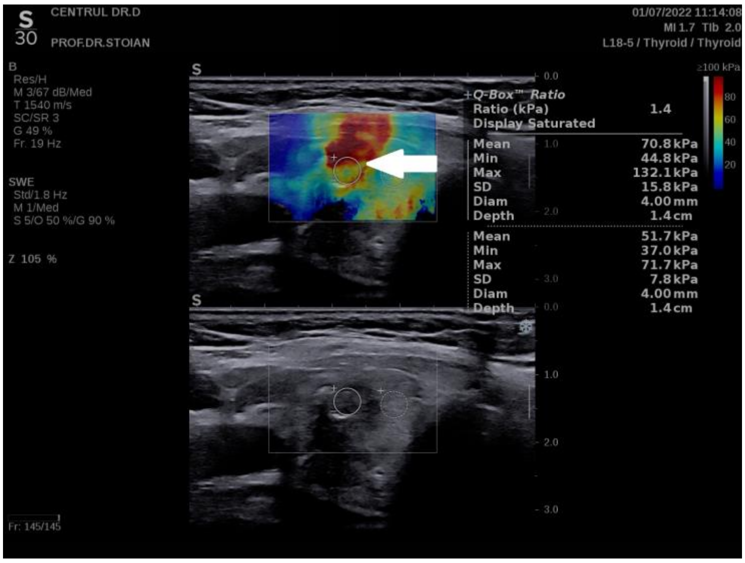

b

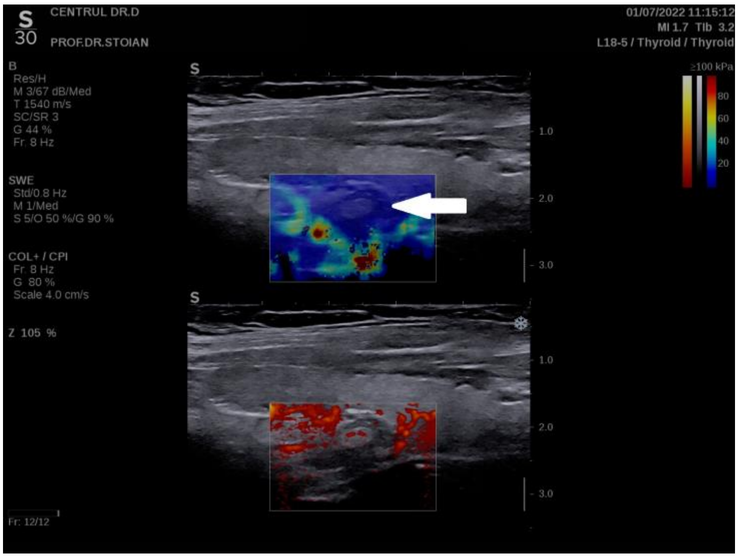

Different neck masses can mimic parathyroid pathology such as: cervical lymph nodes, accessory thyroid lobe, remnant thymus, brachial cyst, thyroglossal cyst, paraganglioma, thyroid nodules located in accessory lobes, or strap muscle tumors. (19) The following figures are presenting the most frequent encountered neck pathologies that could falsely suggest the presence of parathyroid tissue [Figure 27-34].

Figure 27 Right accessory thyroid lobe, isoechoic, with the same pattern as the thyroid parenchyma, pseudo capsule (full arrow) left PTA – well defined, teardrop-shaped, hypoechoic, homogeneous (dash arrow)

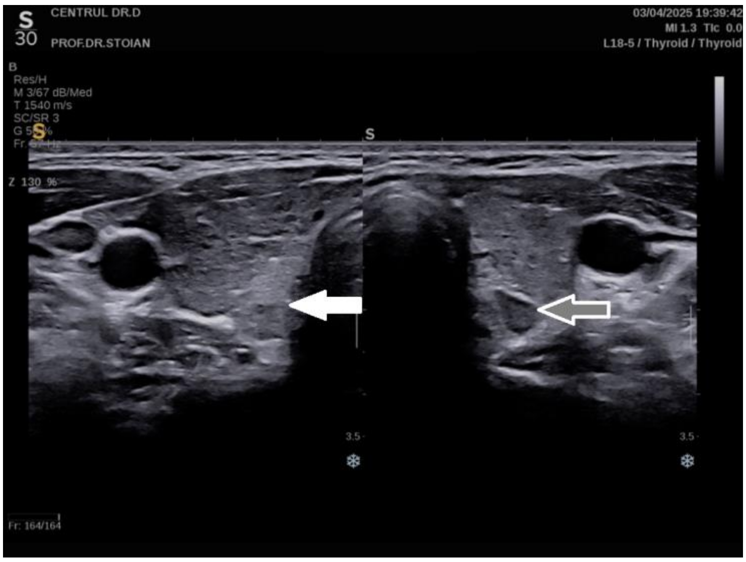

Figure 28 **Transverse section left: left thyroid lobe – jugulo-carotidian lymph node - oval, central hyperechoic hilum (gray arrow) and left superior parathyroid adenoma, round, hypoechoic, homogeneous (white arrow)**.

Figure 29 **Status post thyroidectomy with infrathyroid solid hypoechoic, more echogenic than muscle with “starry sky" appearance due to scattered, bright hyperechoic spots and lines** within it, specific aspect for thymus (white arrow)

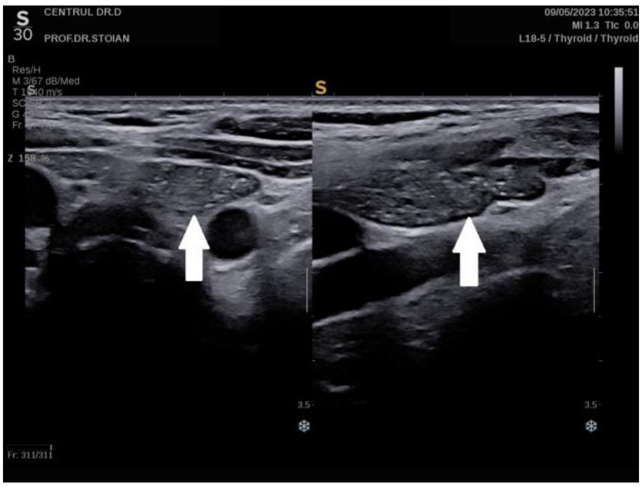

Figure 30 Para midline thyroglossal duct cyst - fluctuant cystic structures which splay the strap muscles with posterior acoustic enhancement – longitudinal section (a) well defined, anterior midline or paramedian location. within 2 cm of the midline, infrahyoid location – transvers section (b).

a

b

Figure 31 Branchial cyst - typically located laterally in the anterior neck, adjacent to the anterior surface of the sternocleidomastoid muscle, and lateral to the carotid space and posterior to the submandibular gland.

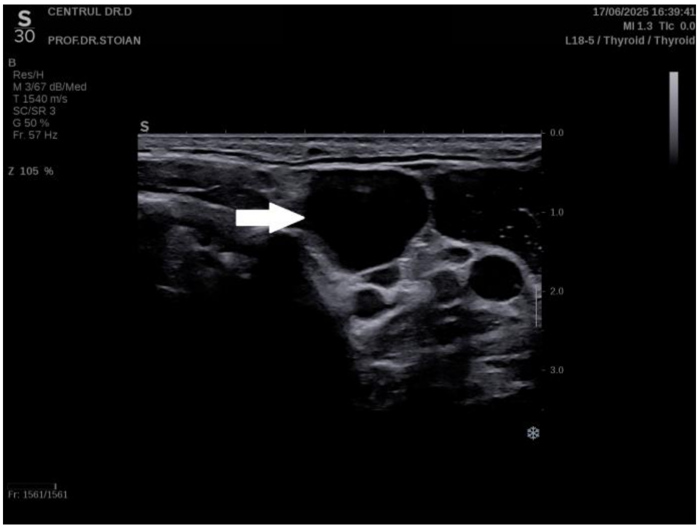

Figure 32 Paramedial suprahyoid nodular lesions, with typical thyroid parenchyma pattern, TIRADS 3 nodule, follicular adenoma confirmed by fine needle biopsy. Transverse section (a). **Longitudinal section (b)**.

a

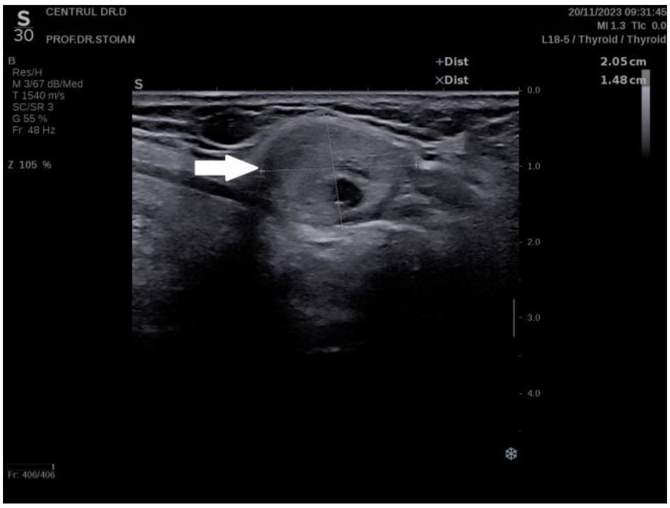

b

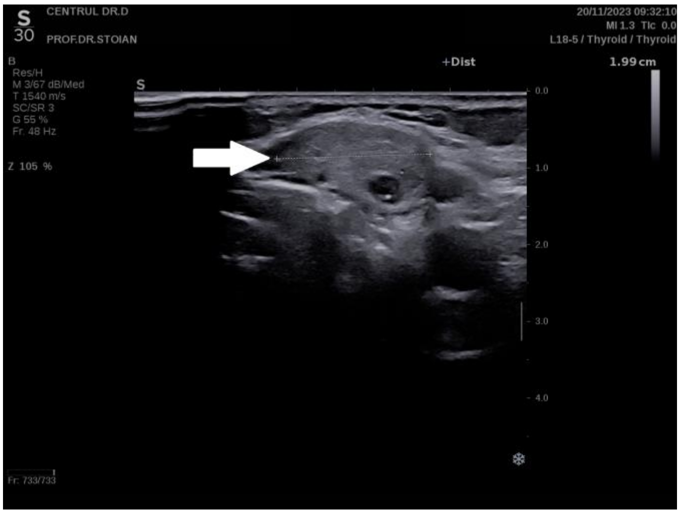

Figure 33 Status post thyroidectomy, left sided, longitudinal scan, multiple solid, hypoechoic, oval, inhomogeneous lesions suggestive for foreign body granuloma.

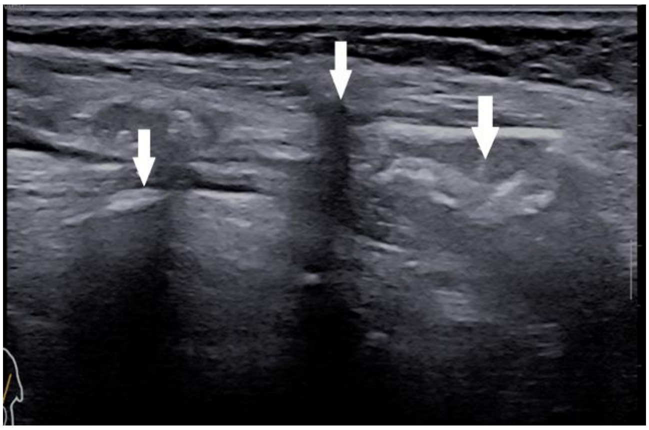

Figure 34 Transverse section- normal thyroid (a). Paramedian homogenous, well defined isoechoic solid lesion – leiomyoma SCLM muscle – right longitudinal section (b).

a

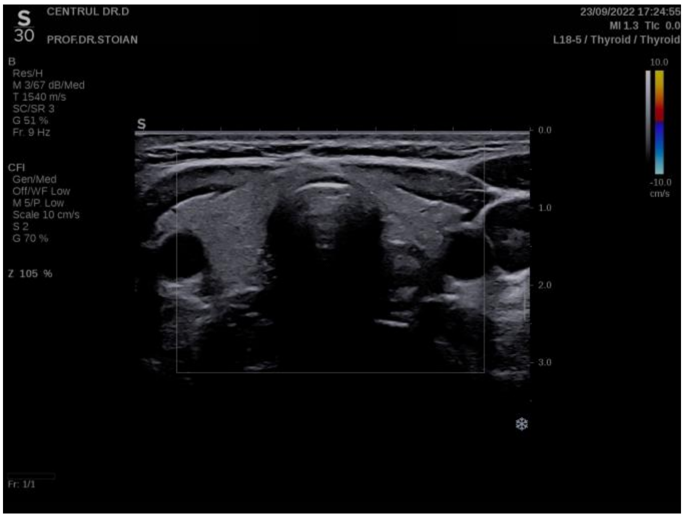

b

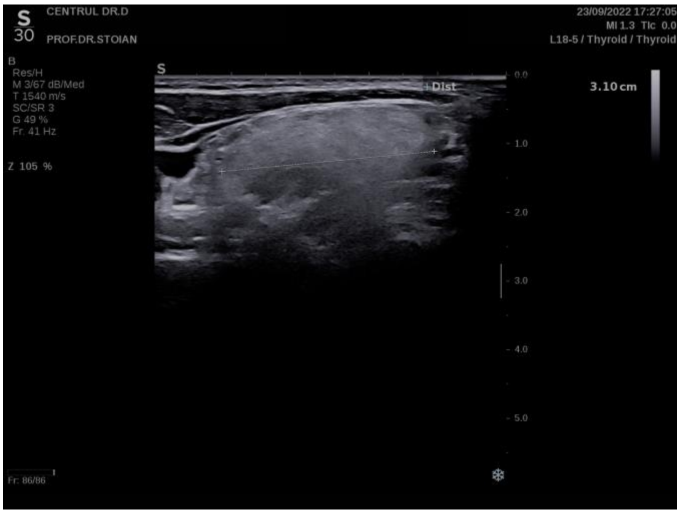

All these pitfalls explain why the morpho-functional diagnostic, in general, ultrasound diagnostic in particular, is recommended only in cases with confirmed hyperparathyroidism both primary and secondary, with a surgical indication (3,4,17).

From the clinical point of view, in cases of incidental ultrasound evaluation, with images suggestive for parathyroid tissue, the questions that need to address are the following:

1. Is it a true parathyroid structure?
2. Is it hyperplastic/hypertrophic, or a normal parathyroid?
3. Is it uni- or multifocal lesion?
4. Adenoma or carcinoma – since it is important to avoid fine needle biopsy in cancer cases, due to increased risk of recurrence following the tumor rupture and seeding (43,44) and

because it is quite important to recognize malignancy prior to surgery because radical resection is required in malignant cases (37,38).

5. Is it concomitant thyroid pathology? - since presence of thyroid disease needs clarification, and surgery, indicated for either thyroid or parathyroid pathology, has to address also the concomitant pathology. Bethesda V or VI categories, molecular anomalies in Bethesda III and IV cases, respectively age below 50, calciuria exceeding 250 mg/day in females, and 300 mg/day in males, and symptoms of end organ impairment are all absolute indications for surgery (1,3,32).

Ultrasound has emerged as a fundamental tool in the diagnostic evaluation of parathyroid disorders, serving as the recommended initial imaging technique due to its safety, absence of ionizing radiation, accessibility, and low cost. High-resolution B-mode ultrasound accurately localizes enlarged parathyroid glands, differentiates them from neighboring thyroid nodules and cervical lymph nodes, and offers essential morphological information that aids in surgical planning. The incorporation of color Doppler imaging facilitates the assessment of vascular patterns, perhaps aiding in the differentiation of parathyroid lesions from other cervical structures.

Recent technical breakthroughs have significantly enhanced the diagnostic capabilities of ultrasonography. The incorporation of elastography provides a quantitative evaluation of tissue rigidity, facilitating the distinction between parathyroid adenomas and atypical parathyroid tumors or carcinomas, which generally have elevated stiffness values. Likewise, contrast-enhanced ultrasonography (CEUS) has shown promise in enhancing lesion characterization through the assessment of microvascular patterns. These multimodal ultrasound techniques have enhanced diagnostic precision and reinforced the significance of ultrasound as an essential element in preoperative localization procedures.

Nonetheless, constraints remain. The efficacy of ultrasound may be influenced by the operator's expertise, the patient's body composition, and the existence of multiglandular disease, ectopic or deeply situated parathyroid tissue, thus necessitating additional imaging modalities like SPECT/CT or 4D-CT for thorough assessment. Notwithstanding these obstacles, when incorporated into a multimodal diagnostic framework, ultrasound markedly increases preoperative planning, promotes less invasive surgical techniques, and ultimately improves clinical outcomes in patients with parathyroid problems.

MCQ

MCQ 1 According to current guidelines, morphological imaging of the parathyroid glands is primarily used for:

1. Establishing the diagnosis of hyperparathyroidism
2. Excluding hyperparathyroidism
3. Preoperative localization in patients with surgical indication
4. Differentiating benign from malignant lesions
5. Screening asymptomatic patients for hyperparathyroidism

Correct answer: 3

MCQ 2 Which of the following statements correctly describes the ultrasound appearance of normal parathyroid glands?

1. Always hypoechoic relative to the thyroid parenchyma
2. Well-defined, homogeneous, iso- or hyperechoic structures
3. Always irregular and heterogeneous in shape
4. Not visualized due to their small size in all cases
5. Detected in 100% of patients during ultrasound examination

Correct answer: 2

According to elastography findings, which statement is correct regarding parathyroid adenomas?

A. They have similar stiffness to malignant thyroid nodules
B. They always exhibit elasticity values above 20 kPa
C. They are stiffer than both benign and malignant thyroid nodules
D. They are generally softer than thyroid tissue
E. Elastography cannot differentiate between adenomas and thyroid lesions

Correct answer: D

Which of the following statements best describes the vascular pattern of parathyroid adenomas on Doppler ultrasound?

A. They are typically avascular lesions

B. They usually exhibit peripheral and intralesional hypervascularity, often with a distinct feeding artery

C. Their vascular pattern is identical to cervical lymph nodes

D. They have no diagnostic features on Doppler imaging

E. Only malignant lesions are vascularized

Correct answer: B

Which combination of features is most suggestive of parathyroid carcinoma on ultrasound?

A. Hyperechoic lesion with a distinct feeding artery

B. Lesion <1 cm, homogeneous, smooth margins

C. Lesion >3 cm, irregular margins, heterogeneous echotexture, and abnormal vascularity

D. Isoechoic lesion, regular margins, peripheral vascular rim

E. Small lesion, intense homogeneous enhancement on CEUS

Correct answer: C

References

1. Bilezikian JP, Khan AA, Silverberg SJ, Fuleihan GEH, Marcocci C, Minisola S, et al. Evaluation and Management of Primary Hyperparathyroidism: Summary Statement and Guidelines from the Fifth International Workshop. J Bone Miner Res. 2022 Nov 1
2. Petranović Ovčariček P, Giovanella L, Carrió Gasset I, Hindié E, Huellner MW, Luster M, et al. The EANM practice guidelines for parathyroid imaging. Eur J Nucl Med Mol Imaging. 2021 Aug 1 [cited 2025 Jul 20];48(9):2801.
3. Overview | Hyperparathyroidism (primary): diagnosis, assessment and initial management | Guidance | NICE.

4. Wilhelm SM, Wang TS, Ruan DT, Lee JA, Asa SL, Duh QY, et al. The American Association of Endocrine Surgeons Guidelines for Definitive Management of Primary Hyperparathyroidism. JAMA Surg [Internet]. 2016 Oct 1;151(10):959.
5. Wu C, Zhu B, Kang S, Wang S, Liu Y, Mei X, et al. Ultrasound characteristics of normal parathyroid glands and analysis of the factors affecting their display. BMC Med Imaging [Internet]. 2024 Dec 1;24(1):1.
6. Marchand JG, Ghander C, Bienvenu-Perrard M, Rouxel A, Buffet C, Russ G. Normal Parathyroid Glands Are Most Often Seen on Neck Ultrasound. Acad Radiol 2024 Sep 1 [cited 2025 Jul 20];31(9):3605.
7. Obara T, Fujimoto Y, Aiba M. Stromal fat content of the parathyroid gland. Endocrinol Jpn. 1990;37(6):901.
8. Cohen SM, Noel JE, Puccinelli CL, Orloff LA. Ultrasound Identification of Normal Parathyroid Glands. OTO Open. 2021 5(4):2473974X211052857.
9. Taterra D, Wong LM, Vikse J, Sanna B, Pękala P, Walocha J, et al. The prevalence and anatomy of parathyroid glands: a meta-analysis with implications for parathyroid surgery. Langenbecks Arch Surg. 2019 Feb 15;404(1):63.
10. Sandakly N, Zreika B, Haddad F, Ghorra C, Abboud B. Supernumerary ectopic parathyroid adenoma in the aortopulmonary window: Navigating diagnostic and surgical challenges. Int J Surg Case Rep. 2025 Jun 1;131:111326.
11. Xia C, Zhu Q, Li Z, Hu M, Fang J, Zhong Q, et al. Study of the Ultrasound Appearance of the Normal Parathyroid Using an Intraoperative Procedure. J Ultrasound Med. 2019 Feb 1
12. Wieneke JA, Smith A. Parathyroid adenoma. Head Neck Pathol. 2008;2(4):305.
13. Yu Q, Hardin H, Chu YH, Rehrauer W, Lloyd R V. Parathyroid Neoplasms: Immunohistochemical Characterization and Long Noncoding RNA (lncRNA) Expression. Endocr Pathol 2019 Jun 15
14. Sporea I, Popescu A, Puiu S, Cela D, Saraci B, Grgurevic I, et al. Integrating Ultrasound into Clinical Practice. 2025.
15. Yazgi D, Richa C, Salenave S, Kamenicky P, Bourouina A, Clavier L, et al. Differentiating pathologic parathyroid glands from thyroid nodules on neck ultrasound: the PARATH-US cross-sectional study. The Lancet regional health Europe. 2023 Dec;35.
16. Morris MA, Saboury B, Ahlman M, Malayeri AA, Jones EC, Chen CC, et al. Parathyroid Imaging: Past, Present, and Future. Front Endocrinol (Lausanne). 2022 Feb 25;12:760419.

17. Zafereo M, Yu J, Angelos P, Brumund K, Chuang HH, Goldenberg D, et al. American Head and Neck Society Endocrine Surgery Section update on parathyroid imaging for surgical candidates with primary hyperparathyroidism. Head Neck. 2019 Jul 1;41(7):2398.
18. Mohammadi A, Moloudi F, Ghasemi-Rad M. Spectral doppler analysis of parathyroid adenoma: Correlation between resistive index and serum parathyroid hormone concentration. American Journal of Roentgenology. 2013 Aug 24;201(2).
19. Centello R, Sesti F, Feola T, Sada V, Pandozzi C, Di Serafino M, et al. The Dark Side of Ultrasound Imaging in Parathyroid Disease. J Clin Med. 2023 Apr 1;12(7):2487.
20. Kunstman JW, Kirsch JD, Mahajan A, Udelsman R. Parathyroid Localization and Implications for Clinical Management. J Clin Endocrinol Metab. 2013 Mar 1;98(3):902–12.
21. Mohammadi A, Moloudi F, Ghasemi-rad M. The role of colour Doppler ultrasonography in the preoperative localization of parathyroid adenomas. Endocr J. 2012 ;59(5):375.
22. Cotoi L, Amzar D, Sporea I, Borlea A, Navolan D, Varcus F, et al. Shear Wave Elastography versus Strain Elastography in Diagnosing Parathyroid Adenomas. 2020.
23. Polat AV, Ozturk M, Akyuz B, Celenk C, Kefeli M, Polat C. The diagnostic value of shear wave elastography for parathyroid lesions and comparison with cervical lymph nodes. Med Ultrason. 2017 Nov 29;19(4):386.
24. Stangierski A, Wolinski K, Ruchala M. Shear wave elastography in the diagnostics of parathyroid adenomas–new application of the method. Endocrine. 2018 May 1 ;60(2):240–5.
25. Girişgen İ, Güngör G, Yüksel S. Evaluation of the Parathyroid Gland using Ultrasound Elastography in Children with Mineral Bone Disorder Due to Chronic Kidney Disease.
26. Amzar D, Cotoi L, Sporea I, Timar B, Schiller O, Schiller A, et al. Shear Wave Elastography in Patients with Primary and Secondary Hyperparathyroidism. J Clin Med. 2021 Feb 2;10(4):1.
27. Azizi G, Piper K, Keller JM, Mayo ML, Puett D, Earp KM, et al. Shear wave elastography and parathyroid adenoma: A new tool for diagnosing parathyroid adenomas. Eur J Radiol. 2016 Sep 1;85(9):1586.
28. Stoian D, Borlea A, Taban L, Maralescu FM, Bob F, Schiller O, et al. Differentiating thyroid nodules parathyroid lesions using 2D-shear-wave elastography: a novel approach for enhanced diagnostic accuracy. Front Endocrinol (Lausanne). 2023;14:1231784.
29. Cotoi L, Amzar D, Sporea I, Borlea A, Navolan D, Varcus F, et al. Shear Wave Elastography versus Strain Elastography in Diagnosing Parathyroid Adenomas. 2020.

30. Amzar D, Cotoi L, Borlea A, Adela C, Pop GN, Stoian D, et al. Role of Elastography in the Evaluation of Parathyroid Disease. Elastography - Applications in Clinical Medicine. 2022 Jul 18.
31. Pavlovics S, Radzina M, Niciporuka R, Ratniece M, Mikelsone M, Tauvena E, et al. Contrast-Enhanced Ultrasound Qualitative and Quantitative Characteristics of Parathyroid Gland Lesions. Medicina (B Aires). 2021 Jan 1;58(1):2.
32. Bilezikian JP. Primary Hyperparathyroidism. J Clin Endocrinol Metab. 2018 Nov 1;103(11):3993.
33. Da Silva NPB, Jung EM, Jung F, Schlitt HJ, Hornung M. VueBox® perfusion analysis of contrast-enhanced ultrasound (CEUS) examinations in patients with primary hyperparathyroidism for preoperative detection of parathyroid gland adenoma. Clin Hemorheol Microcirc. 2018;70(4):423.
34. Aghaa A, Hornung M, Schlitt HJ, Stroszczynski C, Jung EM. The role of contrast-enhanced ultrasonography (CEUS) in comparison with 99mTechnetium-sestamibi scintigraphy for localization diagnostic of primary hyperparathyroidism. Clin Hemorheol Microcirc. 2014;58(4):515.
35. Sidhu PS, Talat N, Patel P, Mulholland NJ, Schulte KM. Ultrasound features of malignancy in the preoperative diagnosis of parathyroid cancer: a retrospective analysis of parathyroid tumours larger than 15 mm. Eur Radiol. 2011 Sep;21(9):1865.
36. Bollerslev J, Schalin-Jäntti C, Rejnmark L, Siggelkow H, Morreau H, Thakker R, et al. Unmet therapeutic, educational and scientific needs in parathyroid disorders: Consensus Statement from the first European Society of Endocrinology Workshop (PARAT). Eur J Endocrinol. 2019 [cited 2025 Jul 26];181(3):P1.
37. Liu R, Xia Y, Chen C, Ye T, Huang X, Ma L, et al. Ultrasound combined with biochemical parameters can predict parathyroid carcinoma in patients with primary hyperparathyroidism. Endocrine. 2019 Dec 1;66(3):673.
38. Liu R, Gao L, Shi X, Ma L, Wang O, Xia W, et al. Shear wave elastography for differentiating parathyroid neoplasms with malignant diagnosis or uncertain malignant potential from parathyroid adenomas: initial experience. Cancer Imaging. 2022 Dec 1;22(1).
39. McCoy KL, Yim JH, Zuckerbraun BS, Ogilvie JB, Peel RL, Carty SE. Cystic parathyroid lesions: functional and nonfunctional parathyroid cysts. Arch Surg. 2009 Jan;144(1):52.

40. Zheng Y xiong, Xu S ming, Wang P, Chen L. Preoperative localization and minimally invasive management of primary hyperparathyroidism concomitant with thyroid disease. J Zhejiang Univ Sci B. 2007;8(9):626.

41. Masatsugu T, Yamashita H, Noguchi S, Nishii R, Watanabe S, Uchino S, et al. Significant clinical differences in primary hyperparathyroidism between patients with and those without concomitant thyroid disease. Surg Today. 2005 May;35(5):351.

42. Cotoi L, Borcan F, Sporea I, Amzar D, Schiller O, Schiller A, et al. Thyroid Pathology in End-Stage Renal Disease Patients on Hemodialysis. Diagnostics. 2020 Apr 1;10(4):245.

43. Harari A, Waring A, Fernandez-Ranvier G, Hwang J, Suh I, Mitmaker E, et al. Parathyroid Carcinoma: A 43-Year Outcome and Survival Analysis. J Clin Endocrinol Metab. 2011 Dec 1;96(12):3679.

44. Parathyroid Carcinoma Presenting as a hyperparathyroid Crisis. Korean J Inter Med. 2012; 27(2):229.